

Received November 17, 2020, accepted November 26, 2020, date of publication December 1, 2020, date of current version December 10, 2020.

Digital Object Identifier 10.1109/ACCESS.2020.3041758

Design of the Broadband Metamaterial Absorber Based on Dispersed Carbon Fibers in Oblique Incidence

LEILEI YAN¹, ZHIHENG HE¹, WEI JIANG², AND XITAO ZHENG¹

¹School of Aeronautics, Northwestern Polytechnical University, Xi'an 710072, China

²National High Performance Integrated Circuit (Shanghai) Design Center, Shanghai 201204, China

Corresponding author: Xitao Zheng (zhengxt@nwpu.edu.cn)

This work was supported in part by the National Natural Science Foundation of China under Grant 11702236, in part by the Aeronautical Science Foundation of China under Grant 201909053001, in part by the Natural Science Basic Research Plan in Shaanxi Province of China under Grant 2020JQ-113, and in part by the Fundamental Research Funds for the Central Universities under Grant G2019KY05106.

ABSTRACT In this paper, a broadband double-layer metamaterial absorber (MMA) based on carbon fibers (CFs) is proposed, which consists of three basic elements. Firstly, the reflectivity of CFs double-layer MMA in normal incidence is analyzed, and compared to the copper double-layer MMA with same size, the simulated results show that it obtains better absorbing effect. With the increase of incident angle, the multi-frequency resonance is activated, leading to larger effective bandwidth. Moreover, when incident angle is between 55 and 70 degrees, the continuous absorption band above 85% can totally cover X and Ku microwave band. Meanwhile, when the EM frequency is at 6-7.5GHz, the change of incident angle hardly affects the absorbing performances of CFs double-layer MMA. A specimen of the CFs double-layer MMA was fabricated by the vacuum molding process to verify its effectiveness and the measured results fitted well with the simulated results. In order to discuss the mechanism of EM absorption, the distribution of E-fields and power loss density were monitored. The results indicate that incident angle effects the distribution of E-fields and the way of absorption to change the absorbing performances. The proposed MMA has potential application prospects in the structural and functional integration design of CFs.

INDEX TERMS Carbon fibers composite, metamaterial absorber, oblique incidence, broadband.


I. INTRODUCTION

The metamaterial absorber (MMA) is an effective structure to achieve stealth performances [1]–[4]. The absorbing performances are determined by the periodic unit of the structure and have almost nothing to do with the material itself. Traditional metamaterial absorbers, whether based on mechanism of electromagnetic (EM) resonance [5]–[9] or artificial surface plasmon polaritons [10]–[13], are mostly fabricated by etching periodic metallic units on a copper-clad glass fibers (GFs) laminate. However, in practical applications, the metallic units glued to the substrate are easy to fall off under loading condition, which would affect its EM and mechanical performances significantly.

Compared with metallic metamaterials, carbon materials also have excellent EM wave absorbing performances, such as carbon nanotubes [14], graphene [15], carbon black [16] and helical carbon fibers [17], which are usually added into

concrete or resin matrix as a common design method of MMA. But the ability of EM regulation depends on carbon materials themselves, so they are not flexible in the design of EM absorber. However, Carbon fibers (CFs), as a kind of carbon materials, has also a series of excellent mechanical properties such as high specific strength, high specific modulus, and fatigue resistance and using it as a reinforcing phase of resin-based composite materials, has shown great potential in aerospace applications [18]–[20].

In recent years, the functional design of CFs composite materials has attracted wide attention from researchers. Rosa *et al* [21], [22] have highlighted that short carbon-fiber-reinforced composites are particularly suitable to design high-performing multifunctional metamaterial absorbers. Meanwhile, the researchers have realized a broad-band five-layer absorbing screen with thickness of 5.5 mm and reflectivity below -20 dB wider than 9 GHz. Most recently, Pang *et al.* [23] proposed a carbon composite metamaterial consisting of the breaking CFs arrays and carbon black to obtain the low-cost broadband and low EM reflection.

The associate editor coordinating the review of this manuscript and approving it for publication was Muhammad Zubair .

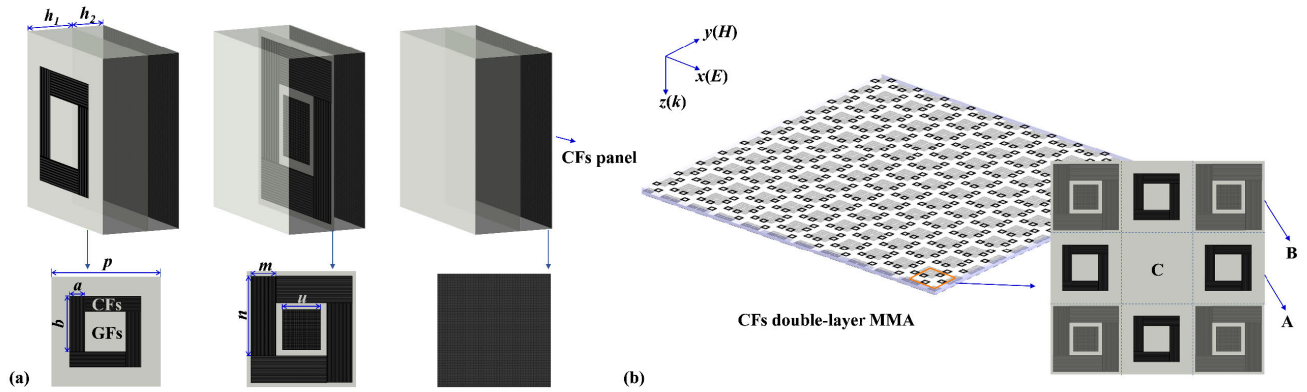


FIGURE 1. (a) The models of three basic elements: they are first-layer CFs square ring element (A), middle-layer CFs square ring, board element (B) and no CFs element (C) from left to right; (b) The CFs double-layer MMA model. Inset is its unit cell consisted of element A, B and C.

TABLE 1. Optimum geometry parameters and material property.

| p | a | b | h ₁ | m | n | u | h ₂ | CFs Conductivity (S/m) | GFs |
|-------|-------|-------|----------------|-----|-----|-----|----------------|---|---|
| 8.7mm | 1.2mm | 4.4mm | 2.4mm | 2mm | 6mm | 3mm | 2.0mm | $\sigma_l = 2.5 \times 10^4$ $\sigma_t = 89$ | $\epsilon = 4.3$ $\tan \delta = 0.025$ |

Jiang *et al.* [24] designed a structure/function integrated sandwich structure with excellent microwave absorption and mechanical properties by using gradient CFs arrays. But they all sew the CFs directly on the substrate without impregnating the resin, which could not make full use of the mechanical properties of the CFs.

In this paper, a broadband CFs double-layer MMA in oblique incidence was designed based on the mechanism of EM resonance. The specimen was made of the unidirectional CFs prepreg and GFs plain weave prepreg and was cured and formed once by vacuum bag process to improve mechanical properties of the interface between CFs and GFs. Meanwhile, the mechanism of absorption was discussed through monitoring E-fields and power loss density. The absorptivity spectrum was drawn to discuss absorption of CFs double-layer MMA in different incident angle.

II. SIMULATIONS AND EXPERIMENT

A. STRUCTURE DESIGN

When EM waves are incident from free space to the interface of MMAs, EM waves are reflected and absorbed without transmission because of the metallic back panel. The EM resonance theory [25]–[27] shows that MMA will meet the impedance matching condition near the resonant frequency, leading to reflect EM waves hardly and achieving a perfect absorbing effect. The flexible design of the periodic unit of the MMA can meet the absorbing requirements of various frequency bands. In 2010, Gu C *et al.* [28] proposed a kind of MMA consisted of metallic ring, plate and parallel metallic ring, which obtain wide-band absorption in the terahertz band through electrical resonance and magnetic resonance provided by the coupling between different

metallic structures. In 2019, Cheng *et al* [29] designed a seven-band polarization-insensitive and wide-angle MMA, composed of a single closed-meander-wire resonator structure that placed over a metallic ground plane by a dielectric substrate, in the microwave frequency region.

In this paper, T300 unidirectional CFs prepreg and GFs plain weave prepreg were as the materials to design three kinds of basic elements, including first-layer CFs square ring element (A), middle-layer CFs square ring, board element (B) and no CFs element (C), as shown in the **Fig. 1 (a)**.

Considering the EM anisotropy of the unidirectional CFs, the CFs board in the middle layer should be two layers laid orthogonally to make the MMA centrosymmetric to ensure polarization-insensitive absorption in the normal incidence. Then the three elements are combined into a 3 × 3 periodic unit with the area ratio of 4:4:1 to constitute the center-symmetric CFs double-layer MMA, as shown in **Fig. 1 (b)**. Due to the diversity of elements, with the increase of incident angle, the multi-frequency resonance will be activated leading to broadband absorbing performances. Meanwhile, the unit size is controlled by 8 parameters and the **Table 1** shows the optimum geometry parameters.

B. SIMULATIONS

EM simulation was performed by using Frequency Domain Solve of CST Microwave Studio 2015. Periodic boundary conditions in x, y directions and open boundary in z direction were applied. The incident wave was set as TM polarized wave, the source type was set as Zmax, the excitation signals were default values and the incident angle was θ , as shown in Fig. 1. The output item was set as S₁₁ to obtain the reflectivity of the metamaterial. If the power of the

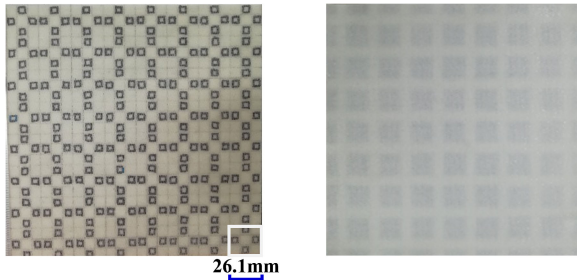


FIGURE 2. The specimen of CFs double-layer MMA (The left is the front and the right is the back).

incident wave is one, the reflectivity R could be calculated by $R(\omega) = 1 - A(\omega) - T(\omega)$ [30]–[32]. However, the transmissivity T should be zero with effect of the CFs back panel, so the absorptivity A can be given by $A(\omega) = 1 - R(\omega)$. The longitudinal and transverse conductivities of the CFs composite were set as 2.5×10^4 and 89 S/m [23], respectively and the permittivity and loss tangent of the GFs composite were set as 4.3 and 0.025, as shown in **Table 1**. Meanwhile, the EM parameters of copper were obtained from that of the copper (annealed) in material library of CST Microwave Studio 2015. In order to get optimum absorbing performances, eight kinds of geometric parameters were set to control effective bandwidth by the parameters sweep method. In order to explore the absorbing mechanism of MMA, the distribution of E-fields and power loss density in normal incidence were monitored respectively.

C. SPECIMEN PREPARATION AND EXPERIMENTAL MEASUREMENT

In order to verify the absorbing performances of the CFs double-layer MMA, a specimen was fabricated. Considering the integrity of unit cells on the boundary, the 208.8×208.8 mm CFs double-layer MMA, consisted of the 8×8 cells, was fabricated by using T300 unidirectional CFs prepreg and GFs plain weave prepreg. Firstly, the required CFs strips and squares were cut out utilizing vernier calipers and scissors. Then the GFs prepreg was laid from the bottom

to the top. After finishing laying the second-layer GFs composite, the grid was divided on the GFs composite according to the size of unit element. CFs square rings and boards of the second layer were laid on the surface. It is worth noting that the CFs board should be two layers laid orthogonally to guarantee the central symmetry of MMA. With the same method, the first-layer GFs composite and CFs square rings were laid on the second layer. Then it was put on a flat mold and an atmospheric pressure was applied on the surface of the structure through vacuum bag, so that the layers were kept tight during curing, which is beneficial to enhance the interlayer mechanical properties of the composite material. At last, it was cured and formed in oven at 150°C for one hour. After cooling and stripping, a CFs double-layer MMA specimen was prepared, as shown in **Fig. 2**.

S_{11} parameters of CFs double-layer MMA in normal incidence were measured by free space method in microwave anechoic chamber. The measurement system is based on the Agilent 8720ET analyzer with three broadband rectangular horn antennas covering from 5.2 to 18 GHz totally.

III. RESULTS AND DISCUSSIONS

As shown in **Fig. 3 (a)**, the black solid line is the simulated reflection curve of CFs double-layer MMA in normal incidence. There are two strong absorbing peaks in the 5.2 to 18.0 GHz frequency range, which are 6.75 and 14.00 GHz respectively. Meanwhile, the relative bandwidth of the absorptivity exceeding 85% in the target bandwidth is 28.6%. The red dotted line in **Fig. 3 (a)** is the simulated reflection curve of the copper double-layer MMA. Obviously, CFs double-layer MMA shows a more superior absorption than metallic ones with the same size in normal incidence.

The simulated and measured reflectivity of the CFs double-layer MMA in normal incidence is shown in **Fig. 3 (b)**. The measured result shows an acceptable agreement with the simulation in the allowable error range. Besides the experimental and fabricated errors, the constructive and destructive additions of the edge scattering of the sub-regions may result

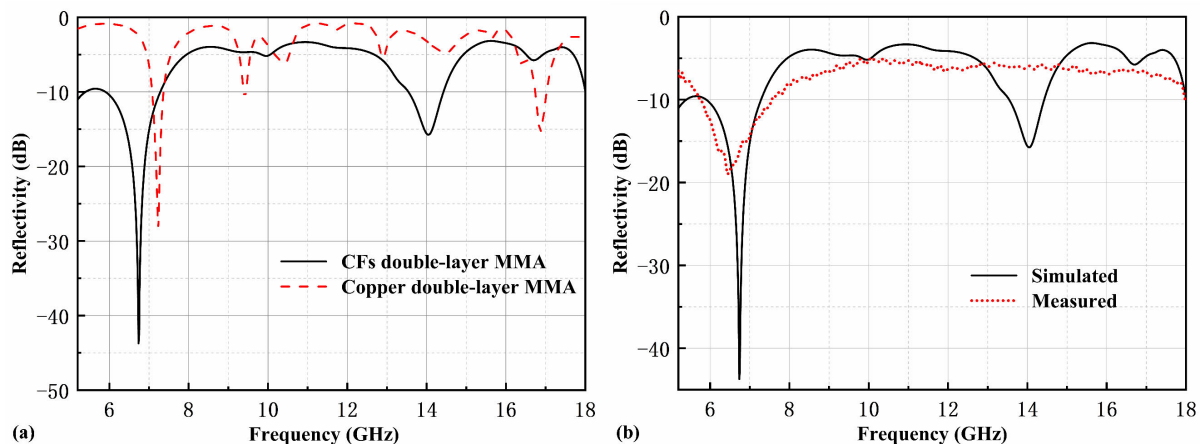


FIGURE 3. CFs double-layer MMA: (a) Comparison with copper double-layer MMA with the same size in the normal incidence; (b) Comparison between the simulated and measured results in the normal incidence.

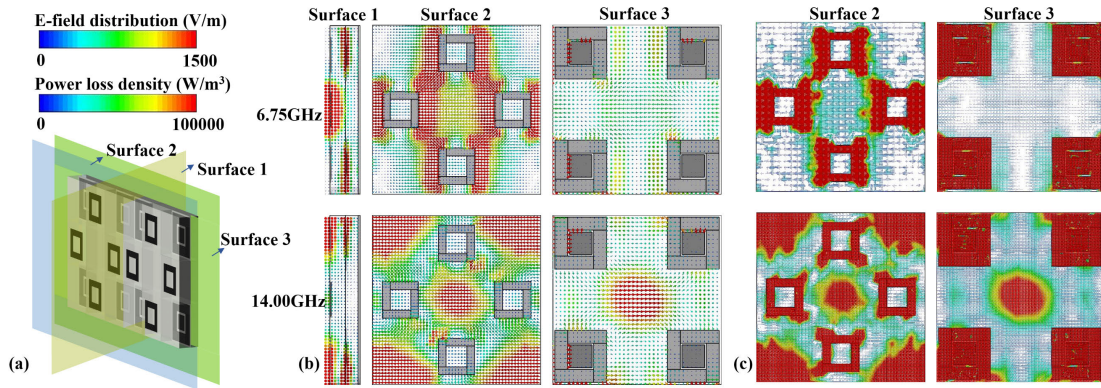


FIGURE 4. Schematic diagram of (a) three monitoring surfaces and the distribution of (b) E-fields (left) and (c) power loss density (right) at 6.75GHz and 14.00 GHz.

in some deviations between the calculated and measured results [33]. But nearby the 14 GHz, there is no strong absorbing peak in the measured results, so it is necessary to explore the reasons for this deviation.

In Fig. 4 (a), three monitoring surfaces were defined. The surface 1 was parallel to the o - y - z plane and located in the center of the adjacent unit cell. The surface 2 and 3 were parallel to the o - y - z plane and located in the interface of the first layer and middle layer between CFs composite and GFs composite respectively. Two resonant frequency points (6.75 GHz and 14.00 GHz) were selected and the monitoring images are shown in Fig. 4 (b, c). The picture on the left of Fig.4 (b) shows the distribution of E-fields on the surface 1. it can be seen that the E-fields at two frequency points are concentrated in the layers where the CFs are located. The middle and right pictures show the E-fields of surface 2 and 3, respectively and the E-fields are polarized around the CFs after entering into the structure. Meanwhile, when the incident frequency is 6.75GHz, areas of locally strong E-fields mainly distributed around CFs, but when it is 14.00 GHz, the local strong E-fields are concentrated on the medium. It is indicated that CFs double-layer MMA responds differently to EM waves of different frequencies. The power loss density in Fig. 4 (c) shows that the loss at 6.75GHz is mainly distributed on CFs, which means that at this frequency, the ohmic loss of CFs absorbs EM wave energy. On the contrary, the loss at 14.00GHz is largely distributed in the GFs composite, so the dielectric loss plays a leading role in the absorption. The loss mechanism of CFs double-layer MMA has changed at different frequencies. Based on analyze above, another reason for deviation about the second absorbing peak is that the loss tangent of GFs composite used for specimen is too small resulting in insufficient medium loss.

In the practical application, the radar wave frequently arrives at the target in oblique incidence, so the absorbing performances of the CFs double-layer MMA in different incident angles were simulated and the absorptivity spectrum was drawn, as shown in Fig. 5. With the increase of the incident angle, new absorbing peaks gradually appeared and the absorbing bandwidth was greatly expanded through the superposition of different absorbing frequency bands.

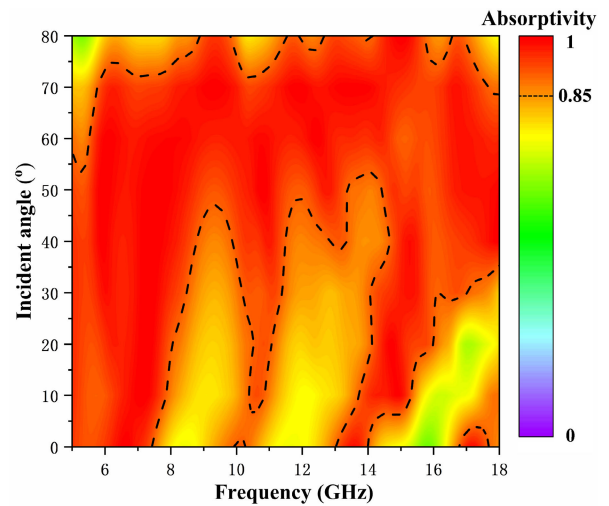


FIGURE 5. The absorptivity spectrum of CFs double-layer MMA for oblique incidence.

When incident angle is between 55 and 70 degrees, the continuous absorption band above 85% can totally cover X and Ku microwave band. Compared with normal incidence, oblique incidence can activate the multi-frequency resonance and achieve broadband wave absorption through ohmic loss and dielectric loss. Meanwhile, when the EM frequency is at 6-7.5GHz, the change of incident angle hardly affects the absorbing performances of CFs double-layer MMA, so it can obtain wide-angle and wide-band absorption, which largely meets the practical application.

IV. CONCLUSION

A CFs double-layer MMA was designed to achieve the broadband absorption in oblique incidence in present study. Three kinds of elements have been considered to constitute the MMA and its absorbing band can totally cover X and Ku microwave band at 55-70 degrees of incidence. Meanwhile, the CFs double-layer MMA has wide-angle absorbing performances at 6-7.5GHz and always guarantees an absorptivity above 85%. The proposed MMA has potential application prospects in load bearing and EM waves absorption.

REFERENCES

- [1] J. Sun, L. Liu, G. Dong, and J. Zhou, "An extremely broad band metamaterial absorber based on destructive interference," *Opt. Exp.*, vol. 19, no. 22, pp. 21155–21162, 2011.
- [2] Y. J. Yoo, S. Ju, S. Y. Park, Y. J. Kim, J. Bong, T. Lim, K. W. Kim, J. Y. Rhee, and Y. Lee, "Metamaterial absorber for electromagnetic waves in periodic water droplets," *Sci. Rep.*, vol. 5, no. 1, Sep. 2015, Art. no. 14018, doi: [10.1038/srep14018](https://doi.org/10.1038/srep14018).
- [3] Q. Zhou, X. Yin, F. Ye, X. Liu, L. Cheng, and L. Zhang, "A novel two-layer periodic stepped structure for effective broadband radar electromagnetic absorption," *Mater. Des.*, vol. 123, pp. 46–53, Jun. 2017, doi: [10.1016/j.matdes.2017.03.044](https://doi.org/10.1016/j.matdes.2017.03.044).
- [4] C.-Y. Wang, J.-G. Liang, T. Cai, H.-P. Li, W.-Y. Ji, Q. Zhang, and C.-W. Zhang, "High-performance and ultra-broadband metamaterial absorber based on mixed absorption mechanisms," *IEEE Access*, vol. 7, pp. 57259–57266, 2019, doi: [10.1109/ACCESS.2019.2913278](https://doi.org/10.1109/ACCESS.2019.2913278).
- [5] B.-X. Wang, X. Zhai, G.-Z. Wang, W.-Q. Huang, and L.-L. Wang, "A novel dual-band terahertz metamaterial absorber for a sensor application," *J. Appl. Phys.*, vol. 117, no. 1, Jan. 2015, Art. no. 014504, doi: [10.1063/1.4905261](https://doi.org/10.1063/1.4905261).
- [6] N. Mishra, D. K. Choudhary, R. Chowdhury, K. Kumari, and R. K. Chaudhary, "An investigation on compact ultra-thin triple band polarization independent metamaterial absorber for microwave frequency applications," *IEEE Access*, vol. 5, pp. 4370–4376, 2017, doi: [10.1109/ACCESS.2017.2675439](https://doi.org/10.1109/ACCESS.2017.2675439).
- [7] H. Zou and Y. Cheng, "Design of a six-band terahertz metamaterial absorber for temperature sensing application," *Opt. Mater.*, vol. 88, pp. 674–679, Feb. 2019, doi: [10.1016/j.optmat.2019.01.002](https://doi.org/10.1016/j.optmat.2019.01.002).
- [8] J. Wu, F. Zhang, Q. Li, J. Chen, Q. Feng, and L. Wu, "Infrared five-band polarization insensitive absorber with high absorptivity based on single complex resonator," *Opt. Commun.*, vol. 456, Feb. 2020, Art. no. 124575, doi: [10.1016/j.optcom.2019.124575](https://doi.org/10.1016/j.optcom.2019.124575).
- [9] Y. Zhang, P. Wu, Z. Zhou, X. Chen, Z. Yi, J. Zhu, T. Zhang, and H. Jile, "Study on temperature adjustable terahertz metamaterial absorber based on vanadium dioxide," *IEEE Access*, vol. 8, pp. 85154–85161, 2020, doi: [10.1109/ACCESS.2020.2992700](https://doi.org/10.1109/ACCESS.2020.2992700).
- [10] F. Ding, Y. Cui, X. Ge, Y. Jin, and S. He, "Ultra-broadband microwave metamaterial absorber," *Appl. Phys. Lett.*, vol. 100, no. 10, Mar. 2012, Art. no. 103506, doi: [10.1063/1.3692178](https://doi.org/10.1063/1.3692178).
- [11] C. Long, S. Yin, W. Wang, W. Li, J. Zhu, and J. Guan, "Broadening the absorption bandwidth of metamaterial absorbers by transverse magnetic harmonics of 210 mode," *Sci. Rep.*, vol. 6, no. 1, Feb. 2016, Art. no. 21431, doi: [10.1038/srep21431](https://doi.org/10.1038/srep21431).
- [12] Y. Pang, J. Wang, H. Ma, M. Feng, Y. Li, Z. Xu, S. Xia, and S. Qu, "Spatial k-dispersion engineering of spoof surface plasmon polaritons for customized absorption," *Sci. Rep.*, vol. 6, no. 1, Jul. 2016, Art. no. 29429, doi: [10.1038/srep29429](https://doi.org/10.1038/srep29429).
- [13] F. Chen, Y. Cheng, and H. Luo, "A broadband tunable terahertz metamaterial absorber based on single-layer complementary gammadion-shaped graphene," *Materials*, vol. 13, no. 4, p. 860, Feb. 2020, doi: [10.3390/ma13040860](https://doi.org/10.3390/ma13040860).
- [14] J. L. Kuang, X. J. Hou, T. Xiao, Y. Li, Q. Wang, P. Jiang, W. B. Cao, "Three-dimensional carbon nanotube/SiC nanowire composite network structure for high-efficiency electromagnetic wave absorption," *Ceram. Int.*, vol. 45, pp. 6263–6267, Apr. 2019.
- [15] X. Zhang, X. Wang, P. Sha, B. Wang, Y. Ding, and S. Du, "High-efficiency electromagnetic wave absorption of epoxy composites filled with ultralow content of reduced graphene/carbon nanotube oxides," *Compos. Sci. Technol.*, vol. 189, Mar. 2020, Art. no. 108020, doi: [10.1016/j.compscitech.2020.108020](https://doi.org/10.1016/j.compscitech.2020.108020).
- [16] R. Jan, M. B. Khan, and Z. M. Khan, "Synthesis and electrical characterization of 'carbon particles reinforced epoxy-nanocomposite' Ku-band," *Mater. Lett.*, vol. 70, pp. 155–159, Mar. 2012.
- [17] S. Xie, Z. Ji, B. Li, L. Zhu, and J. Wang, "Electromagnetic wave absorption properties of helical carbon fibers and expanded glass beads filled cement-based composites," *Compos. A, Appl. Sci. Manuf.*, vol. 114, pp. 360–367, Nov. 2018.
- [18] J.-K. Kim and Y.-W. Mai, "High-strength, high fracture-toughness fiber composites with interface control—A review," *Compos. Sci. Technol.*, vol. 41, no. 4, pp. 333–378, 1991, doi: [10.1016/0266-3538\(91\)90072-W](https://doi.org/10.1016/0266-3538(91)90072-W).
- [19] S. Chand, "Carbon fibers for composites," *J. Mater. Sci.*, vol. 35, pp. 1303–1313, Mar. 2000, doi: [10.1023/A:1004780301489](https://doi.org/10.1023/A:1004780301489).
- [20] S.-S. Yao, F.-L. Jin, K. Y. Rhee, D. Hui, and S.-J. Park, "Recent advances in carbon-fiber-reinforced thermoplastic composites: A review," *Compos. B, Eng.*, vol. 142, pp. 241–250, Jun. 2018, doi: [10.1016/j.compositesb.2017.12.007](https://doi.org/10.1016/j.compositesb.2017.12.007).
- [21] I. M. De Rosa, F. Sarasini, M. S. Sarto, and A. Tamburrano, "EMC impact of advanced carbon fiber/carbon nanotube reinforced composites for next-generation aerospace applications," *IEEE Trans. Electromagn. Compat.*, vol. 50, no. 3, pp. 556–563, Aug. 2008.
- [22] I. M. De Rosa, R. Mancinelli, F. Sarasini, M. S. Sarto, and A. Tamburrano, "Electromagnetic design and realization of innovative fiber-reinforced broad-band absorbing screens," *IEEE Trans. Electromagn. Compat.*, vol. 51, no. 3, pp. 700–707, Aug. 2009.
- [23] Y. Q. Pang, Y. F. Li, J. F. Wang, M. B. Yan, S. B. Qu, S. Xia, and Z. Xu, "Electromagnetic reflection reduction of carbon composite materials mediated by collaborative mechanisms," *Carbon*, vol. 147, pp. 112–119, Jun. 2019.
- [24] W. Jiang, H. Ma, J. Wang, J. Yang, L. Yan, Y. Fan, and S. Qu, "Spoof surface polaritons realized by unidirectional carbon fibers arrays and applications in structure/function integrated sandwich structure," *Results Phys.*, vol. 17, Jun. 2020, Art. no. 103081.
- [25] J. Lee, M. Yoo, and S. Lim, "A study of ultra-thin single layer frequency selective surface microwave absorbers with three different bandwidths using double resonance," *IEEE Trans. Antennas Propag.*, vol. 63, no. 1, pp. 221–230, Jan. 2015, doi: [10.1109/TAP.2014.2365826](https://doi.org/10.1109/TAP.2014.2365826).
- [26] B. X. Khuyen, B. S. Tung, N. V. Dung, Y. J. Yoo, Y. J. Kim, K. W. Kim, Y. D. Lam, J. G. Yang, and Y. Lee, "Size-efficient metamaterial absorber at low frequencies: Design, fabrication, and characterization," *J. Appl. Phys.*, vol. 117, no. 24, Jun. 2015, Art. no. 243105, doi: [10.1063/1.4923053](https://doi.org/10.1063/1.4923053).
- [27] N. I. Landy, S. Sajuyigbe, J. J. Mock, D. R. Smith, and W. J. Padilla, "Perfect metamaterial absorber," *Phys. Rev. Lett.*, vol. 100, May 2008, Art. no. 207402.
- [28] C. Gu, S. B. Qu, and Z. B. Pei, "A wide-band, polarization-insensitive and wide-angle terahertz metamaterial absorber," *Prog. Electromagn. Res. Lett.*, vol. 12, pp. 171–179, Jan. 2010.
- [29] Y. Cheng, Y. Zou, H. Luo, F. Chen, and X. Mao, "Compact ultra-thin seven-band microwave metamaterial absorber based on a single resonator structure," *J. Electron. Mater.*, vol. 48, no. 6, pp. 3939–3946, Jun. 2019.
- [30] S.-J. Li, P.-X. Wu, H.-X. Xu, Y.-L. Zhou, X.-Y. Cao, J.-F. Han, C. Zhang, H.-H. Yang, and Z. Zhang, "Ultra-wideband and polarization-insensitive perfect absorber using multilayer metamaterials, lumped resistors, and strong coupling effects," *Nanoscale Res. Lett.*, vol. 13, no. 1, p. 386, Nov. 2018, doi: [10.1186/s11671-018-2810-0](https://doi.org/10.1186/s11671-018-2810-0).
- [31] S. J. Li, T. J. Cui, Y. B. Li, C. Zhang, R. Q. Li, X. Y. Cao, and Z. X. Guo, "Multifunctional and multiband fractal metasurface based on inter-metamolecular coupling interaction," *Adv. Theory Simul.*, vol. 2, no. 8, Aug. 2019, Art. no. 1900105, doi: [10.1002/adts.201900105](https://doi.org/10.1002/adts.201900105).
- [32] S. J. Li, Y. B. Li, H. Li, Z. X. Wang, C. Zhang, Z. X. Guo, R. Q. Li, X. Y. Cao, Q. Cheng, and T. J. Cui, "A thin self-feeding janus metasurface for manipulating incident waves and emitting radiation waves simultaneously," *Annalen der Physik*, vol. 532, no. 5, May 2020, Art. no. 2000020, doi: [10.1002/andp.202000020](https://doi.org/10.1002/andp.202000020).
- [33] Y.-C. Hou, W.-J. Liao, C.-C. Tsai, and S.-H. Chen, "Planar multi-layer structure for broadband broad-angle RCS reduction," *IEEE Trans. Antennas Propag.*, vol. 64, no. 5, pp. 1859–1867, May 2016, doi: [10.1109/TAP.2016.2535164](https://doi.org/10.1109/TAP.2016.2535164).



LEILEI YAN received the B.Eng. degree in materials science and engineering from Xi'an Jiaotong University, in 2008, and the Ph.D. degree in solid mechanics, in 2014.

He is currently an Associate Professor with the School of Aeronautics, Northwestern Polytechnical University, Xi'an, China. From September 2008 to March 2014, he studied at the State Key Laboratory for Mechanical Structure Strength and Vibration, Xi'an Jiaotong University. From 2014 to 2018, he works as a Lecturer with Air Force Engineering University. In July 2018, he became an Associate Professor, continuing his scientific interests in solid mechanics. He has authored or coauthored more than 20 SCI articles in materials and mechanics journals, and his works have been cited over 200 times.



ZHIHENG HE was born in Han Zhong, Shaanxi, China, in 1997. He received the B.S. degree in aircraft design and engineering from Northwestern Polytechnical University, Xian, China, in 2019, where he is currently pursuing the M.S. degree in solid mechanics.

Since 2019, he is a member of the Institute of Aircraft Composite Structure, Northwestern Polytechnical University. His research interests include metamaterial absorber, lightweight composite structure design, and structure optimization. His awards and honors include “Xu Zhilun Excellent Student Award in Mechanics of China Society” in 2018 and the champion of RTM group in the 12th China SAMPE Ultralight Composite Wing Student Competition.



WEI JIANG was born in Nantong, Jiangsu, China, in October 1991. He received the Ph.D. degree in electronic science and technology from Shandong University, in June 2020. He is mainly focused on the research of multifunctional metamaterials. He is currently an Assistant Researcher with the National High Performance Integrated Circuit Design Center, Shanghai, China.



XITAO ZHENG received the Ph.D. degree in solid mechanics, in 2003.

He is currently the Director of the Institute of Aircraft Composite Structure, Northwestern Polytechnical University, where he is a Professor with the School of Aeronautics. He has been engaged in the research of structural mechanical behavior of aviation composite materials for more than 30 years, and has presided over more than 50 projects including the National Natural Science Foundation of China, the Aviation Science Foundation, the AVIC Industry-University-Research Innovation Fund, International Cooperation Projects, Shaanxi Science Foundation, and pre-research projects. He coauthored two monographs *Advanced Composite Material Aircraft Structure Design and Application* and *Fatigue Characteristics of Composite Laminates*, co-translated one book *Commercial Aircraft Composite Material Technology*, edited one textbook, in More than 130 papers have been published in academic journals and conferences at home and abroad, and six Chinese patents. His awards and honors include one second prize and three third prizes of provincial and ministerial level scientific and technological progress, one first prize of Shaanxi University Science and Technology Prize and Contribution Award of the 7th Education Working Committee of the Chinese Society of Mechanics.

...